



# Development of a flexible strain sensor from graphite-treated fabric for smart applications

Nisreen AlAtrash <sup>1</sup>•, Ghazal Tuhmaz <sup>2</sup>• and Ziad Saffour <sup>3</sup>•.

<sup>1,2,3</sup>Spinning and textile department- Faculty of chemical and petroleum engineering- Homs University- Homs- Syria

•These authors contributed equally to this work

DOI: <http://doi.org/10.29194/NJES.29010111>

Received: September 15, 2025

Revised: December 14, 2025

Accepted: December 26, 2025

Published: March 20, 2026

## Abstract

This research is based on developing a flexible strain sensor from graphite-treated fabric using knife coating technology. Three sensors were formed, differing in the number of coating layers (2, 4, 6). The results of studying their properties had shown that with increasing a number of coating layers, the electrical conductivity value of the treated samples increased, reaching a value of  $(21.8 \times 10^{-3} \text{ S/cm})$ . The treated layer was superficial, as the penetration of the coating into the structure did not increase significantly. It was also shown that the treatment did not affect the fabric properties such as hardness and tear strength. When studying the sensor's performance, it was found that the sensor's resistance value changes with the change in its bending angle. The change rate was higher for the six-layer sample, and the response time was shorter, faster (0.8s), than the other samples. Then, a working system was applied to the sensor to give a command to turn the LED on or off by bending the sensor and it showed good performance. This, in turn, confirms the effectiveness of applying this sensor in smart wearable textiles.

**Keywords:** *Flex Strain Sensor, Graphite, Knife Coating, Smart Fabric, Technical Fabric.*

**Corresponding author:** Provide the corresponding author information and publisher here. E-mail address: [nsreenalatrash89@gmail.com](mailto:nsreenalatrash89@gmail.com)

## 1. Introduction

The textile market has experienced substantial growth in recent years, driven by the introduction of new fibers, fabrics, and innovative processing techniques. This expansion has significantly contributed to technological advancements, beginning with pioneering research in the late 1990s that focused on integrating conductive circuits and wires into textiles [1]. Recent developments in textile research have led to major breakthroughs in the early 2000s [2], including the introduction of the first semiconductor electronic textile components. Additionally, the incorporation of sensors, actuators, system interfaces, and complex textile circuits has greatly enhanced the functionality of smart electronic textiles [3]. The term e-smart textiles refer to a broad field of studies and approaches that expand the functionality and utility of common fabrics. E-smart textiles are textile products such as fibers and yarns with woven, knitted, or non-woven structures that enable them to interact with the environment/user, process the resulting information, and respond to it in an appropriate manner and timeframe [4,5,6]. Smart textiles enhance social welfare and may significantly reduce the social welfare budget due to their high level of intelligence [7]. The primary applications of smart electronic textiles include sensors and

wearable electronics, such as actuators, power generators, and energy storage devices, particularly in the medical field [8,6], health monitoring of vital signs in the human body encompasses parameters such as temperature humidity and heart rate. Electronic textiles provide several benefits, including lightweight design, flexibility, and breathability, all while retaining a softness comparable to traditional fibers and textiles. These innovative materials also incorporate electronic functionalities, making them effective portable devices for tracking essential health parameters [8], various sensors, such as mechanical pressure sensors, strain gauges, and positional sensors, can be integrated with elastic sensors. The functionality of an elastic sensor is based on modifications in its bending angle, which trigger specific commands. Therefore, it is essential to assess the performance of each type of smart textile resistance device through laboratory testing, focusing on their behavior under electrical, mechanical, and thermal condition [9,10]. The primary focus in the smart textile industry is to develop conductive textiles. The overarching goal of smart textiles is to transform all relevant components, such as sensors, actuators, and transmission lines, into fully textile materials. Traditional textiles are inherently non-conductive, requiring conversion to achieve conductivity. Previously, fine metallic threads and fibers were introduced into fabrics, primarily

for anti-static treatment. A significant advancement in textile manufacturing is the development of conductive coatings or inks that are applied to fabrics, allowing for the creation of conductive textiles. This process can take place at various stages of fabric production, including thread formation, weaving, or final finishing operations. The resulting textiles can be either fully conductive or possess conductivity only on their surface [11,12]. The coating being prepared must exhibit electrical conductivity, which requires the inclusion of electrically conductive materials such as metals like silver, copper, gold, and aluminum. The selection of a specific metal often depends on considerations such as cost and availability. It is also important to note that there are non-metallic materials that can achieve electrical conductivity. Activated carbon compounds include graphite, graphene, and carbon nanotubes, as well as conductive polypyrrole and polyaniline [13,14]. However, most researchers have turned to the use of graphite in treating fabrics because it is a revolutionary material that has good electrical, mechanical and thermal properties, and also because of its abundance, low price and the fact that it is largely safe to work with. They have been creative in developing its uses in coating techniques and in the uses of nanofibers and plasma [15] to obtain a technical fabric with many applications (smart electronic fabric, flame-retardant fabric for halogenated compounds, water-repellent fabric and many others). For this reason, this research has been directed to use graphite as a conductive material within the recipe of conductive coating to obtain a conductive fabric [15,16]. Graphite was chosen for this research due to its abundance, low cost, and relative safety. Coated textiles, which involve the application of coating technology to fabrics, have attracted significant attention in the realm of wearable electronics. Coating technology is defined as the process of applying a layer of coating material to the surface of a fabric. This layer is superficial and does not penetrate deeply into the fabric's structure. Various methods are employed to produce and manufacture a wide range of coated fabrics, which can be categorized into several techniques: knife coating, spray coating, roller coating, transfer coating, immersion coating, and both flat and circular screen coating [17, 18]. The research utilizes a knife coating method, a specific type of diffusion coating technique. In this process, a dry and smooth fabric is positioned over a carrier, and the coat is dispensed in front of the knife using either a scoop or a pump, spreading evenly across the width of the fabric before being moved beneath the knife [18]. A locally manufactured laboratory knife coating device was used. Its operating principle is a knife that moves across the surface of the fabric, passing the paint evenly over the entire surface. The fabric sample is fixed to a glass plate with a special fixing mechanism at its ends, as shown in Fig.1.

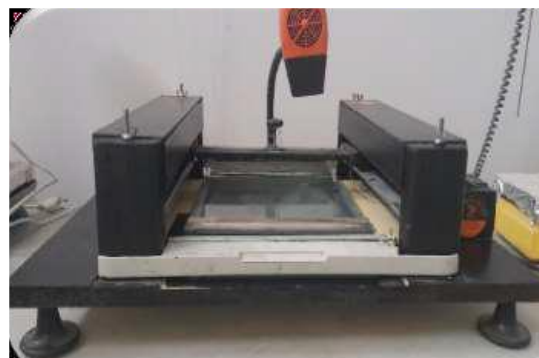


**Figure 1.** Laboratory knife covering device

This research focuses on developing a fabric sensor treated with flexible graphite using the knife coating technique, which involves applying multiple layers of graphite-containing coating on a blended polyester/cotton fabric. This text outlines the specifications, characteristics, and applications of a flexible sensor that alters its resistance in response to changes in its bending angle. Notably, this sensor can be utilized in various applications, including a glove for the deaf and mute that facilitates communication through sign language, as well as smart devices that enable remote on/off control for individuals with disabilities [19,20], among other uses.

## 2. Materials and methods:

### 2.1. Materials:

Cotton/ polyester blend fabric (65/35), 1/2 twill assembly from local market, graphite, distilled water, urea ( $\text{CH}_4\text{N}_2\text{O}$ ), sodium alginate ( $\text{NaC}_6\text{H}_7\text{O}_6$ ), Arduino circuit, LED light.

### 2.2. Coating preparation:

The carrier coating is prepared for application to the fabric by mixing the basic components mentioned in Table 1 in a mixing and homogenizing device at a speed of 8000 rpm for three minutes.

**Table 1.** Proportions of the components in the conductive coating:

Ingredients	Amount (%)
Conductive material(graphite)	5%
Dispersing agent (distilled water)	10%
Thickener (sodium alginate)	0.5%
Hygroscopic agent (urea)	10%
Complete the ratio to 100% with distilled water	74.5%

### 2.3. Fabric treatment with conductive coat using knife-coating technique:

At this stage, a coating treatment is applied to the mixed cotton/polyester fabric using a laboratory knife-coating device. This device functions by securely placing the fabric between two ends of a smooth, flat glass plate, utilizing a specialized tensioning mechanism, a total of 2 ml of coating is evenly poured across the entire width of the sample in front of the knife. The device is then running to move the knife back and forth over the fabric surface, ensuring that the coat is distributed uniformly. This procedure is conducted at a speed of 0.2 cm/sec, requiring a total of 8 strokes, this is followed by the stage of drying the samples with hot air using air dryer. Thus, the first layer of coating has been applied to the

fabric. This process is repeated according to the number of coating layers to be applied to the treated fabric, which ranges from 2 to 6 layers. Fig.2 shows the sequence of the process for applying one layer of coating.

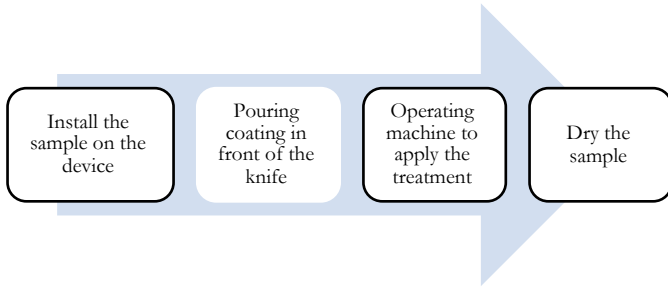


**Figure. 2.** shows the sequence of the process of applying coating to the fabric.

**2.4. Description of treated fabric:**

The treated fabric samples were characterized by several tests as follows

**2.4.1. Calculating the penetration rate of coating into the fabric:**

Determining this ratio is essential for understanding the percentage of coating that penetrates the fabric. This measurement serves as a key indicator in the research, as the treatment technique applied to the fabric is designed to be superficial. Ideally, The coating should ideally remain primarily on the surface of the fabric to minimize significant penetration into its structure, preventing it from reaching the opposite side. The method used to measure the electrical conductivity of the samples is superficial; this means that the probes used to detect conductivity are located on the surface of the treated fabric. For accurate readings, it is essential that the coating containing the conductive material particles remains predominantly on the surface. Therefore, a lower level of penetration results in a thicker surface layer with higher conductivity The penetration rate is calculated based on the following relationship (1) [21]:

$$p = \frac{R_{max} - R}{R_{max} - R_{min}} * 100 \dots \dots, (1)$$

R= Reflection coefficient on the back of the coated fabric.

R<sub>max</sub> = Reflection coefficient of non-coated fabric.

R<sub>min</sub>= Reflection coefficient on the coated face of the fabric.

Fig.3 shows the places where it is measured in coated fabrics.

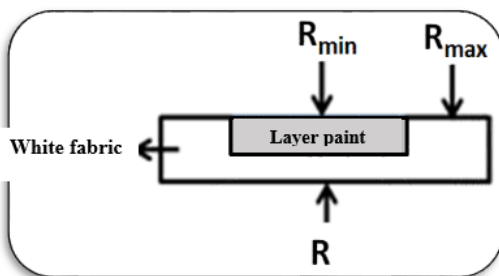


**Figure 3.** Reflection coefficient measured in coated fabrics

When (R=R<sub>min</sub>), the amount of coating on the back side is equal to the amount on the top coated side, and the penetration is complete (P=100%). When (R=R<sub>max</sub>), this means that the coating layer remains on the coated surface, and there is no penetration, and the back side remains white (P=0) [21]. The three reflection

coefficient values were measured for each sample using a spectrophotometer (Triax-550-Jobin Yvon).

**2.4.2. Electrical conductivity:**

The treated samples were characterized in terms of electrical conductivity using a four-probe device manufactured by SIGNATURE Company. whose probes act as sensors to measure the electrical resistance value according to the following relationships (2), (3) [22]:

$$\rho = G * t * \frac{V}{I} \dots \dots \dots (2)$$

ρ: is the value of the specific resistance and is estimated at (Ω.cm).

G: A constant value taken from the table attached to the device according to the length and width of the sample and the measuring distance of the probes.

V/I: The value of the average resistance, which is taken from the slope of the straight line formed from the voltage values resulting from the input current intensity and is estimated as Ω.

t: The coating thickness within the sample estimated in cm.

$$\sigma = 1/\rho \dots \dots \dots (3)$$

σ: Electrical conductivity value is estimated at S.cm<sup>-1</sup>.

Five voltage readings were taken at different current levels, and an average resistance value was calculated, considering the layer thickness and the distance between the probes.

**2.4.3. Loading ratio:**

The percentage of coating loading on the fabric is calculated. In this test, the percentage of dry coat loading on the fabric is calculated by weighing the sample before and after coating in a specific area and applying the relationship (4).

Dry loading ratio =

$$\frac{\text{Sample weight after coating} - \text{Weigh the sample before coating}}{\text{Weigh the sample before loading}} \times 100 \dots \dots \dots (4)$$

**2.4.4. Hardness test:**

This test is performed on treated samples to observe the effect of treatment on the stiffness and bending resistance of the fabric sample. The principle of this test is based on the fabric’s ability to form a cantilever (a support fixed at one end) before bending under its own weight. The test is performed according to the American standard specification (ASTM D1388-2002). The test is performed based on the following steps:[23]

1- Three samples were prepared from each treated sample to conduct three readings for each sample, where each sample had dimensions of (2.5cm) width and (20cm) length.

2- Each sample was placed on a horizontal plane so that the edge of the test sample coincides with the edge of the horizontal plane, then a graduated ruler was placed over the test sample.

3- The ruler was pushed forward and pushes with it towards the sample. Push was continued until the edge of the sample meets the diagonal line at an angle of (41.5°). The reading was recorded of the ruler after a time ranging from (6) to (8) seconds. The reading of the ruler is the bending length of the sample.

4- The stiffness of the fabric is calculated by applying the following relationship:[24]

$$G = K * C^3 * W \dots \dots \dots (5)$$

G: Fabric hardness (g.m).

C: Bending length (m)

W: weight per square meter (g/m<sup>2</sup>).

K: constant, as it is calculated from the relationship:

$$K = \frac{\cos^{\frac{1}{2}}\theta}{8 \tan \theta} \dots \dots \dots (6)$$

θ: bending angle

**2.4.5. Tear strength test:**

The tear strength test was carried out on the samples using the MOO6B testing device, a product of a Chinese company, in order to measure the durability of the fabric after treatment, and to study the effect of the treatment applied on the tear strength of the samples. This was done using a tear strength tester consisting of two jaws, one fixed and the other movable. A slit is made in the sample and then the two ends of the torn sample are placed between the jaws of the device. We show that the test was conducted according to the standard specification ASTM D5587-15 (2019).[25]

**2.4.6.SEM Morphological Characterization:**

Scanning electron microscopy images were taken using a VEGALLXMU microscope made in the Czech Republic of the treated sample to observe how the coating was deposited on the surface.

**3.Discussion of results and application of the sensor:**

**3.1. Penetration rate:**

It is noted from Table (2) and Fig.4 that with the increase in the number of layers, the penetration rate increased to a certain extent and then began to decrease. This is explained by the fact that with the increase in the graphite layers, an impermeable layer was formed on the surface of the fabric, and thus the fabric will not absorb the coated layers after that. This in turn reduces the penetration rate of the coat into the fabric and forms an overlap of layers on the surface, thus resulting in a higher density of the conductive material on the surface. This result is good for the required property because the treatment is superficial (surface application of the coating), and thus the electrical conductivity is higher.

**Table 2.** Results of calculating the penetration rate:

Sample number	∇ Layers	ξ Layers	∩ Layers
Rmin	0.00411	0.00189	0.00165
Rmax	0.01019	0.01019	0.01019
R	0.00885	0.00839	0.00906
P%	22%	21%	13,2%

**3.2. Electrical conductivity:**

he results presented in Table 3 and Fig 5 indicate that increasing the number of coating layers on the fabric surface leads to higher electrical conductivity. This finding aligns with the calculated penetration ratio, which reveals that adding more layers causes the coating to overlap on the surface. As a result, the density of the conductive material on the surface increases, thereby enhancing electrical conductivity. It is important to note that the measured conductivity reflects the surface conductivity of the fabric. The more conductive layer on the surface, the greater the electrical conductivity of the samples

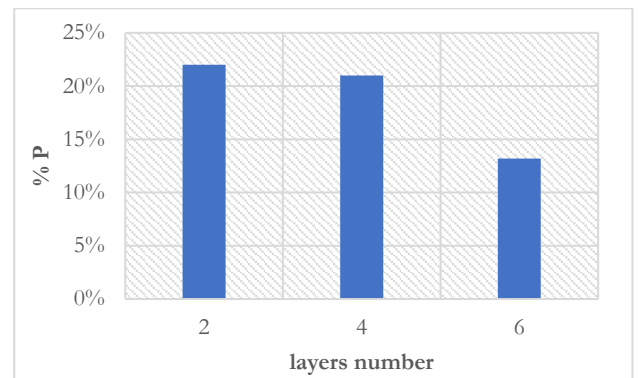


**Figure 4.** shows the penetration percentage values with varying numbers of paint layers.

**3.3. Loading percentage results:**

It was noted from the results shown in Table (4) and Fig.6 that with the increase in the number of layers, the percentage of coating loading on the surface increased, and this is logical because the amount of coating applied increased and thus the weight of the sample increased after loading.

**3.4. Hardness test results:**

Table (5) and Fig.7 show the results of the hardness test for the treated samples and compares them with the reference (untreated) sample. The test procedure was taken for each treated sample three times, the bending length was calculated, and then the average bending length for the three readings was found and applied in the hardness coefficient relationship. It was observed from the results of this test that with the increase in the number of layers, the hardness of the treated samples increased. This is due to the increase in the weight per square meter of the samples with the increase in layers. This in turn affects the value of the hardness coefficient because it is affected by the value of the weight per square meter of the sample.

**Table 3.** Results of measuring electrical conductivity

Sample number	2 Layers	4 Layers	6 Layers
Electrical resistance R*10 <sup>6</sup> (Ω)	40	4	1
Paint thickness within the sample t (cm)	0.01036	0.01298	0.01401
Correction factor(G)	3.2721	3.2721	3.2721
Quality resistance P*10 <sup>+3</sup> (Ω.cm)	1.35600	0.16990	0.04586
Electrical conductivity σ*10 <sup>-3</sup> (S.cm <sup>-1</sup> )	0.737	5.89	21.8

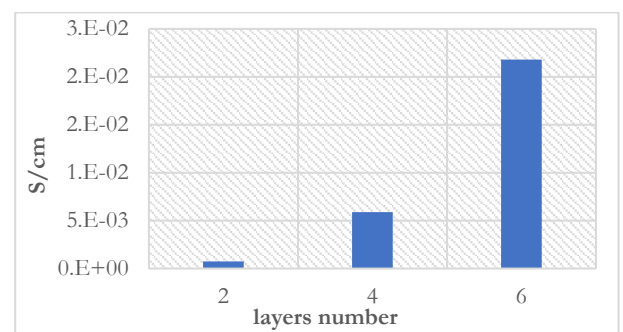


**Figure5.** The electrical conductivity values with varying numbers of coating layers.

**Table 4.** Loading ratio results:

Sample number	weight before coating (gr)	Weight after coating (gr)	loading ratio%
2 layers	0.251	0.296	18%
4 layers	0.251	0.328	31%
6 layers	0.251	0.35	40%

**Table 5.** Hardness test results for fabric samples

Sample number	Untreated	2 layers	4 layers	6 layers
Bend length (m)	0.03	0.08	0.105	0.113
K	0.132	0.132	0.132	0.132
Weight per square meter	251	296	328	350
Hardness factor G(g.m)	0.0009	0.020	0.050	0.067

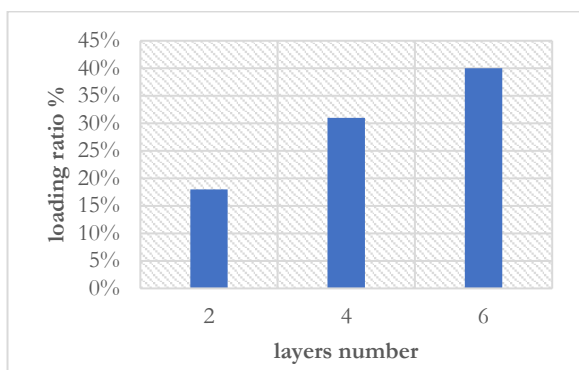


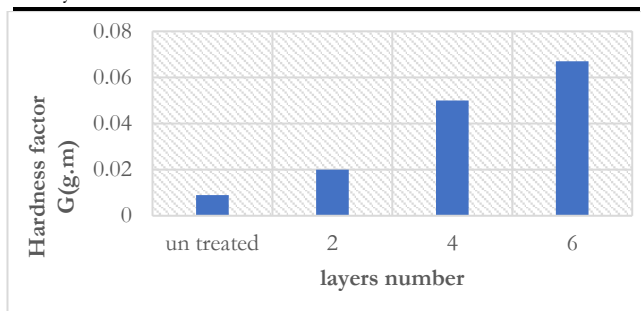
**Figure 6.** The load-bearing ratio values of the treated fabric with varying numbers of paint layers.

**3.5. Tear strength test results:**

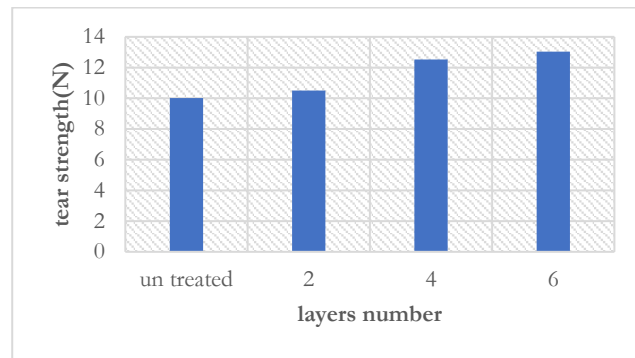
Table 6 and Fig.8 shows the results of the tear strength test for the treated samples and their comparison with the untreated reference sample. Three readings were taken for each sample on the tear strength device and the average tear strength was calculated. It is shown from the results of Table 6 that the applied treatment process did not negatively affect the tear strength of the samples, but on the contrary, it increased. This can be attributed to the fact that the applied coating layers increased the bonding and adhesion of the fibers to each other, which increased tear strength.

**Table 6.** Tear strength test results:

Sample number	Average tear strength(N)	Standard deviation value
0 (Untreated)	10.01	0.015
2 layers	10.5	0.4
4 layers	12.53	0.4
6 layers	13.04	0.16



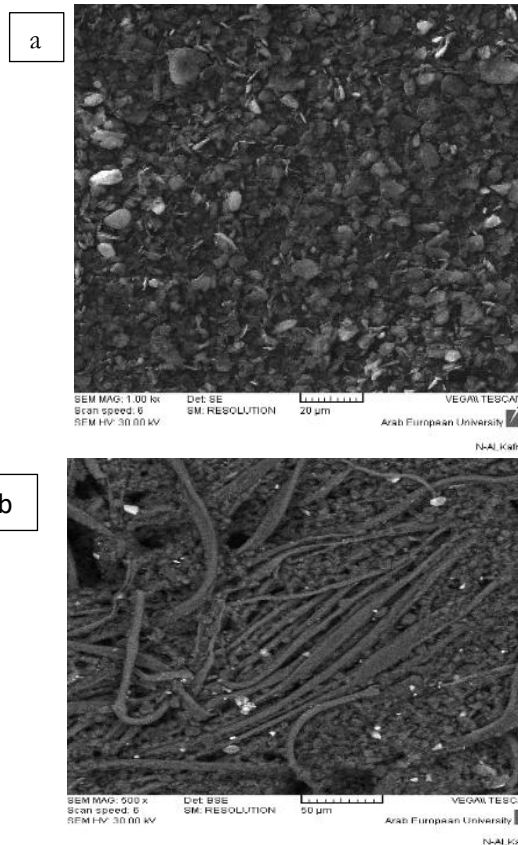
**Figure 7.** The values of the stiffness modulus of the treated fabric with varying numbers of coating layers.



**Figure 8.** The tear strength values of the treated fabric with varying numbers of coating layers

**3.6. SEM:**

Fig (9) shows optical microscope images of graphite powder and graphite-treated fabric. It is clear from Fig (9-a) that the graphite powder has a sheet-like structure, not spherical granules. Fig (9-b) shows how the conductive material is distributed within the fabric structure and how it is positioned and penetrates the yarn deeply and systematically. Fig (9-c) illustrates how the paint is distributed continuously and uniformly across the entire surface of the canvas without any unpainted areas.



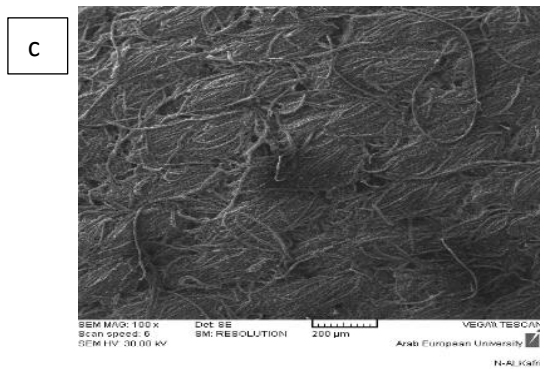


Figure 9. shows scanning electron microscope images where (a) is an image of graphite powder and (b,c) is an image of fabric treated with six layers of graphite

3.7. Flexible sensor application:

1) In order to apply a flexible sensor from the treated fabric Fig.10, a preliminary test must be conducted to ensure that this type of treated fabric can be applied in the form of a flexible sensor. This was done by studying the change in electrical resistance with the change in the bending angle of the treated sample, A slice of the treated sample was cut with dimensions of (1 x 7 cm), and then a protractor was installed to measure the bending angle. Then the two ends of the sample were fixed to the sockets of the electrical resistance measuring device to read the resistance value when the bending angle changed Fig.11, Fig.12 The results were as shown in the diagram in Fig.13, Where the change in resistance is calculated based on the following relationship [26,27]:

$$\Delta R = \frac{R_0 - R_f}{R_0} \dots \dots \dots (7)$$

$\Delta R$ : The change in resistance

$R_0$ = The initial electrical resistance value at an angle of 180 and is estimated( $\Omega$ )

$R_f$ : The value of electrical resistance at each variable angle and is estimated( $\Omega$ ).



Figure 10. shows a picture of the sensor formed from the treated



Figure 11. shows how to measure the change in angle with a change in resistance.

The diagrams in Fig 7 were formed by measuring the electrical resistance of the treated sample in the initial state at an angle of 180° and then bending the sample at an angle of 135. and applying the relationship (7) to calculate the rate of change of resistance for each sample and each angle where we calculate the change at angles (180°-135°-90°-45°). As a result, it was observed that the two-layer

graphite-treated sample had a resistance change rate of 0.03, while the four-layer sample had a resistance change rate of 0.06, and the six-layer sample had a resistance change rate of 0.2. Thus, it is clear that as the conductivity of the treated samples increases, the resistance change rate increases, thereby improving the sensitivity and performance of the sensor.



Figure 12. shows how to measure the change in while applying it to the finger.

The sensor sample was fixed to the finger to measure the response time, and the two ends of the sensor were connected to the two ends of an electrical resistance-measuring device. and the time it takes for the sample's resistance to change with the angle was monitored., the response time of each sensor was calculated when its bending angle changed. The resistance was measured in the initial state at an angle of 180, then the angle was changed and the time taken by the sample to start changing its resistance value was calculated. The bending performance was applied to the finger in order to apply stress to the sample to achieve the sensor's goal of flexible stress. As for the angle formed by the finger, it was measured using the Image program, where pictures of the finger were taken in three cases and the angles formed were measured. The result of that was the diagrams shown in Fig.14, where the sample treated with six layers of graphite the samples with the highest conductivity were more sensitive to angle changes, with a shorter response time than the other samples with lower conductivity. This suggests that the higher the conductivity of the sample, the faster the sensor's response time.

The sensitivity coefficient was calculated based on the reference [28] by calculating the slope of the relationship between angle changes and electrical resistance changes, as illustrated by the diagrams in Fig (15,a,b,c). The slope for the sensors and regression coefficients were found to be ( 0.52 k $\Omega$ / $\theta^\circ$  ,  $R^2=0.9852$ ) for the sensor with six layers of coating, (0.28 k $\Omega$ / $\theta^\circ$  ,  $R^2=0.9888$ ) for the sensor with four layers of coating, and (0.22 k $\Omega$ / $\theta^\circ$  ,  $R^2=0.9671$ ) for the sensor with two layers of coating. Therefore, the sensitivity coefficient for the sensor with six layers is the highest, These results are good compared to other studies that used embroidery and printing to obtain flexible sensors [26][29].

2) A practical test of the formed sensor by applying the sensor in an Arduino circuit in order to turn on and off an LED based on the change in the bending angle of the sensor. In this step, a set of electronic parts is needed to form an operating circuit (Arduino circuit, LED, connecting wires, battery), and that is shown in Figures (16 and 17).

The images in Fig.17 illustrate the principle of applying the sensor in an LED on/off circuit. A board was used to install the LED

light and wires to connect the sensor terminals; in addition to an Arduino (Nod Mcu V3) The Arduino board is a development device specific to the Arduino platform. Its advanced features and compact size, making it suitable for small businesses, characterize it. What distinguishes it from other Arduino versions is its built-in Wi-Fi (wireless network connectivity), multi-use ports (SPI, I2C, ADC, GPIO, UART, PWM), it can be programmed using the Arduino software in the C++ programming language.[30]. The Arduino program gives the command to turn the LED on when the sensor is bent and to turn the LED off when the sensor is left straight. This was done by utilizing the readings of resistance changes given by the sensor when bending, where the electrical resistance value decreased, and when straightening, where the resistance value was higher. Then, these readings were programmed into on/off commands for the LED via the Arduino, as each change in resistance corresponds to an on/off command for the LED. The sensor showed good performance and a quick response.

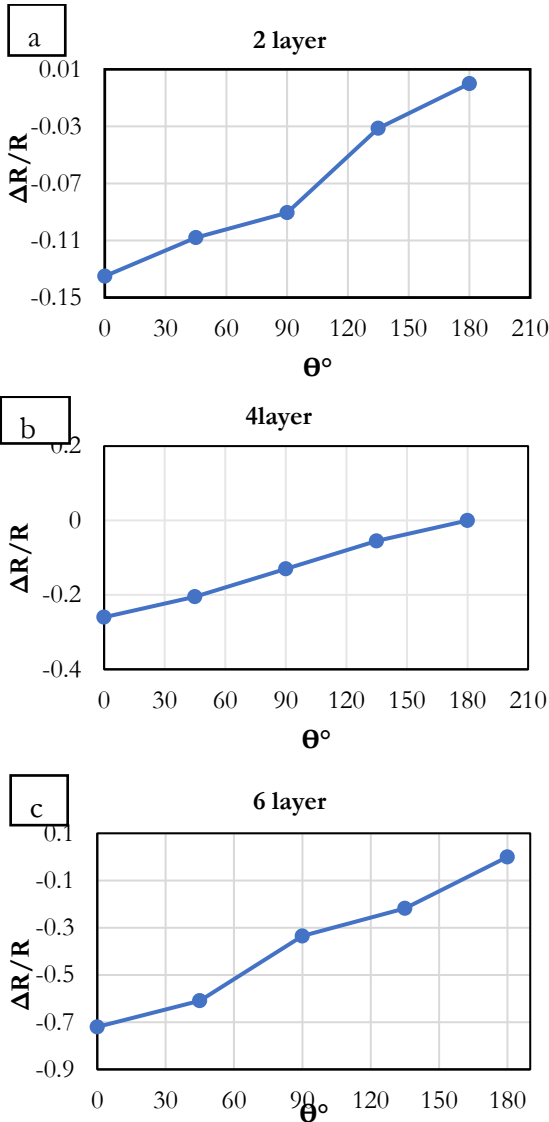


Figure 13. shows the percentage change in electrical resistance with changing sensor angle. Where (a) is the sensitive sample treated with 2 layers of graphite coating, (b) is the sensitive sample treated with 4 layers of graphite, and (c) is the sensitive sample treated with 6 layers of graphite.

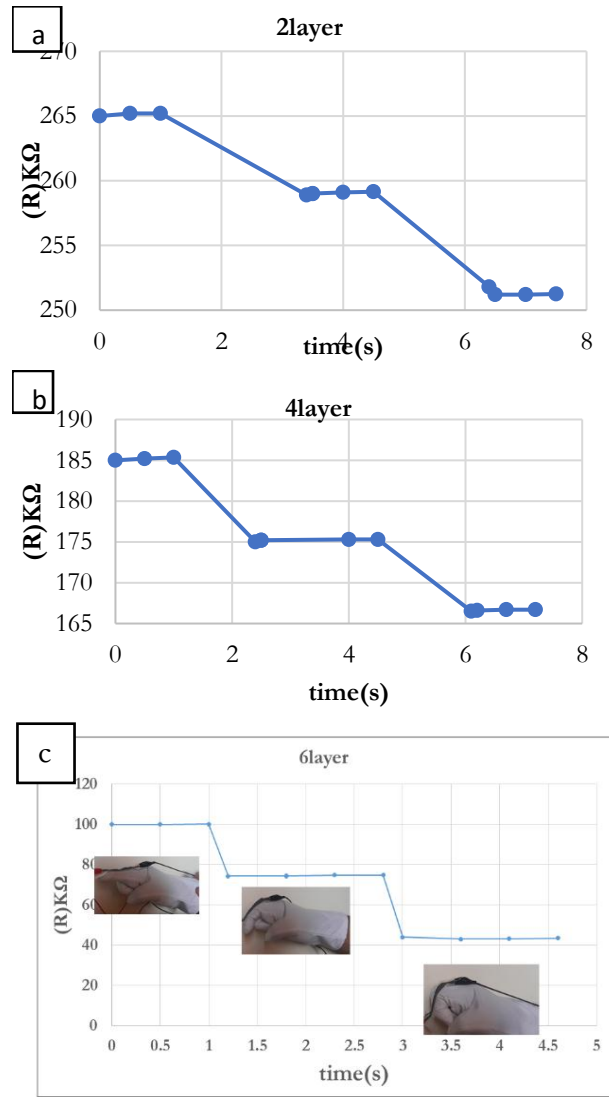
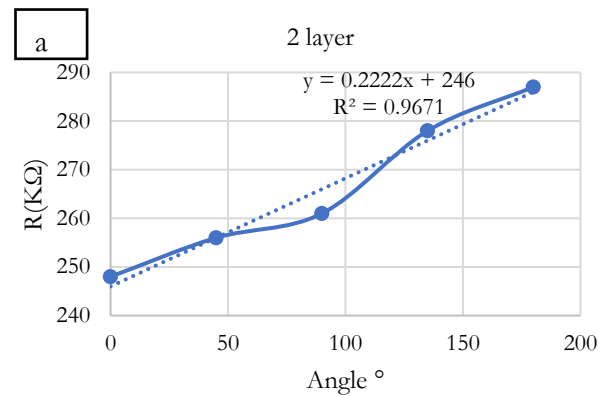


Figure 14. shows the time taken for the sample to change resistance as the sensor angle changes.



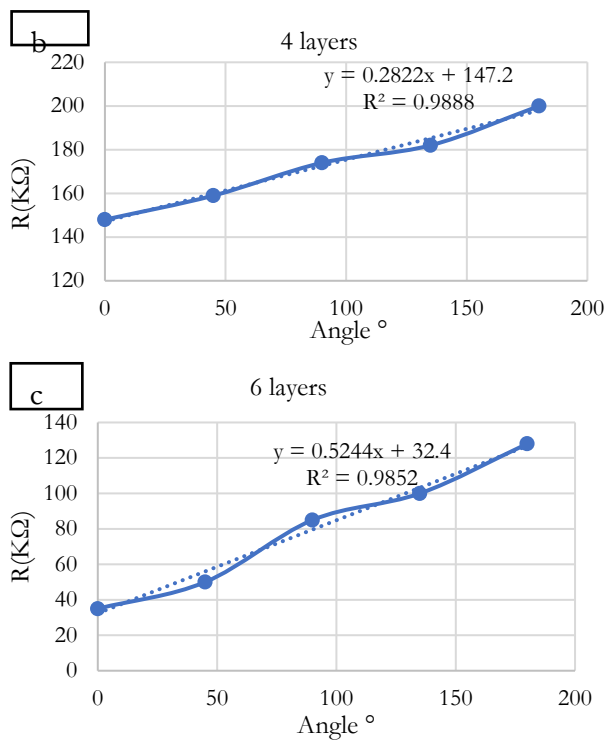


Figure 15. The calculation diagrams for the sensitivity coefficient of sensors.

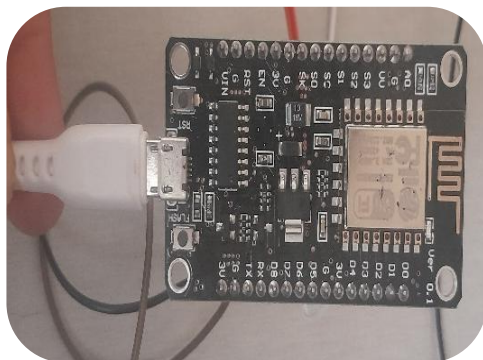


Figure 16. Arduino circuit

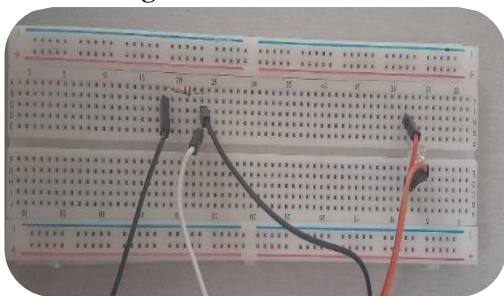


Figure 17. LED mounting plate and wiring

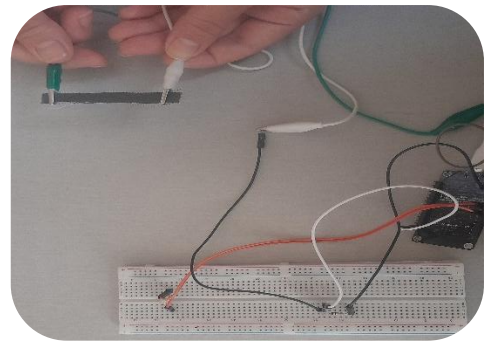
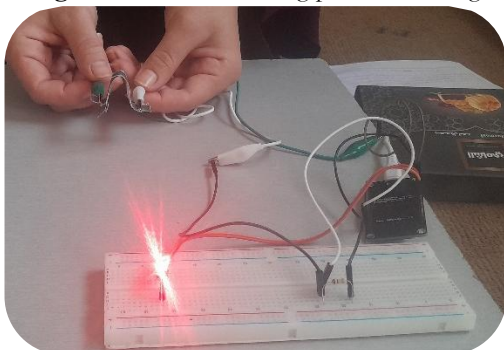


Figure 18. Experiment with the sensor turning the LED on and off.

**4. Conclusions:**

This study was able to develop a flexible stress sensor from graphite-treated fabric, where the knife coating treatment technique was used with graphite-containing coating. Then, the samples treated with two, four and six layers of graphite were characterized in terms of the coating penetration rate and electrical conductivity. It was found that with the increase in the coating layers, the penetration rate did not increase, but rather the treatment was superficial and highly conductive. It can also be also found that the graphite treatment technique for the fabric did not affect the fabric properties but rather increased the tear strength of the treated samples compared to the untreated reference sample. When studying the sensor performance, it was found that the sample with the highest conductivity had a greater percentage of resistance change than the samples with the lowest conductivity, The response time was also faster, meaning that the sample treated with six layers showed a response time of 0.8 seconds, with its resistance value changing when the sensor angle changed. Then, the sensor from the sample treated with six layers was applied to a hand on/off system to ensure its performance and provide good effectiveness and response.

**5. Acknowledgment:**

The authors contributed to the design and implementation of the research, the analysis of the results, and the writing of the manuscript. The authors would like to thank the head of the Department of Spinning and Textile at Petrochemical College at Homs University for his support and cooperation

**6. References:**

[1] G. B. Tseghai, D. A. Mengistic, B. Malengier, K. A. Fante, and L. Van Langenhove, "PEDOT:PSS-based conductive textiles and their applications," *Sensors*, vol. 20, no. 7, p. 1881, 2020. <https://doi.org/10.3390/s20071881>

[2] L. M. Castano and A. B. Flatau, "Smart fabric sensors and e-textile technologies: a review," *Smart Mater. Struct.*, vol. 23, no. 5, p. 053001, 2014. <https://doi.org/10.1088/0964-1726/23/5/053001>

[3] A. Chauraya, R. Seager, W. Whittow, S. Zhang, and Y. Vardaxoglou, "Embroidered frequency selective surfaces on textiles for wearable applications," in *Proc. Loughborough*

- Antennas & Propagation Conf. (LAPC), Loughborough, UK, Nov. 2013, pp. 388-391.  
<https://doi.org/10.1109/LAPC.2013.6711926>
- [4] M. R. Islam, S. Afroj, K. S. Novoselov, and N. Karim, "Smart electronic textile-based wearable supercapacitors," *Adv. Sci.*, vol. 9, no. 31, p. 2203856, 2022.  
<https://doi.org/10.1002/advs.202203856>
- [5] W. Zhang, S. Luan, M. Tian, L. Qu, X. Zhang, T. Fan, and J. Miao, "Smart wearable fibers and textiles: status and prospects," *Nanoscale*, vol. 17, no. 39, pp. 22733-22762, 2025.  
<https://doi.org/10.1039/D5NR02801A>
- [6] M. R. Azani and A. Hassanpour, "Electronic textiles (E-textiles): types, fabrication methods, and recent strategies to overcome durability challenges (washability & flexibility)," *J. Mater. Sci.: Mater. Electron.*, vol. 35, no. 29, p. 1897, 2024.  
<https://doi.org/10.1007/s10854-024-13347-0>
- [7] M. Stoppa and A. Chiolerio, "Wearable electronics and smart textiles: a critical review," *Sensors*, vol. 14, no. 7, pp. 11957-11992, 2014.  
<https://doi.org/10.3390/s140711957>
- [8] B. Younes, "Smart E-textiles: a review of their aspects and applications," *J. Ind. Text.*, vol. 53, p. 15280837231215493, 2023.  
<https://doi.org/10.1177/15280837231215493>
- [9] L. Capineri, "Resistive sensors with smart textiles for wearable technology: from fabrication processes to integration with electronics," *Procedia Eng.*, vol. 87, pp. 724-727, 2014.  
<https://doi.org/10.1016/j.proeng.2014.11.748>
- [10] E. Skrzetuska and P. Rzeźniczak, "Circularity of smart products and textiles containing flexible electronics: challenges, opportunities, and future directions," *Sensors*, vol. 25, no. 6, p. 1787, 2025.  
<https://doi.org/10.3390/s25061787>
- [11] H. Qu and M. Skorobogatiy, "Conductive polymer yarns for electronic textiles," in *Electronic Textiles*, Amsterdam, The Netherlands: Elsevier, 2015, pp. 21-53.  
<https://doi.org/10.1016/B978-0-08-100201-8.00003-5>
- [12] S. Dalvand, A. Foroozandeh, A. Heydarian, F. S. Nasab, M. Omidvar, N. Yazdanfar, and A. A. Asghari, "A review on carbon material-metal oxide-conducting polymer and ionic liquid as electrode materials for energy storage in supercapacitors," *Ionics*, vol. 30, no. 4, pp. 1857-1870, 2024.  
<https://doi.org/10.1007/s11581-024-05426-3>
- [13] S. Maity and A. Chatterjee, "Conductive polymer-based electro-conductive textile composites for electromagnetic interference shielding: review," *J. Ind. Text.*, vol. 47, no. 8, pp. 2228-2252, 2018.  
<https://doi.org/10.1177/1528083716670310>
- [14] A. M. Shana, F. Nasr, M. Abo Aly, and S. A. El-Shafai, "Electrochemical oxidation of textile dye house wastewater using graphite (Gr) and modified graphite (Gr/CuO & Gr/ZnO) electrodes," *Egypt. J. Chem.*, vol. 68, no. 11, pp. 425-440, 2025.  
<https://doi.org/10.21608/ejchem.2025.350682.11193>
- [15] P. Schäl, I. J. Junger, N. Grimmelsmann, and A. Ehrmann, "Development of graphite-based conductive textile coatings," *J. Coat. Technol. Res.*, vol. 15, no. 4, pp. 875-883, 2018.  
<https://doi.org/10.1007/s11998-017-0024-5>
- [16] C. Alonso, A. Manich, A. D. Campo, P. Felix-De Castro, N. Boisseree, L. Coderch, and M. Martí, "Graphite flame retardant applied on polyester textiles: flammable, thermal and in vitro toxicological analysis," *J. Ind. Text.*, vol. 51, no. 3 Suppl., pp. 4424S-4440S, 2022.  
<https://doi.org/10.1177/15280837211062056>
- [17] A. K. Sen, *Coated Textiles: Principles and Applications*. Lancaster, PA, USA: Technomic Publishing Co., 2007.  
<https://doi.org/10.1201/9781420053463>
- [18] W. Fung, *Coated and Laminated Textiles*. Cambridge, UK: Woodhead Publishing, 2002, vol. 23.  
<https://doi.org/10.1533/9781855737518>
- [19] J. Henderson, J. Condell, J. Connolly, D. Kelly, and K. Curran, "Review of wearable sensor-based health monitoring glove devices for rheumatoid arthritis," *Sensors*, vol. 21, no. 5, p. 1576, 2021.  
<https://doi.org/10.3390/s21051576>
- [20] B. O'Flynn, J. T. Sanchez, J. Connolly, J. Condell, K. Curran, P. Gardiner, and B. Downes, "Integrated smart glove for hand motion monitoring," in *Proc. Int. Conf. Sensor Device Technol. Appl.*, May 2015.
- [21] S. Saffour, *Printing Technology: Theoretical Part*. Homs Univ. Publ., 2017.
- [22] M. Neama, "Preparation of polypyrrole sensor by ultrasonic spraying," M.Sc. thesis, Higher Inst. Appl. Sci. Technol., 2016.
- [23] R. Salamon, "The development of types of textile to be used in the production of solar cells," Ph.D. dissertation, Faculty of Chem. & Petrol. Eng., Al-Baath Univ., 2021.
- [24] B. P. Saville, *Physical Testing of Textiles*, ch. 10, "Objective evaluation of fabric handle," Cambridge, UK: Woodhead Publ. Ltd., 1999.  
<https://doi.org/10.1533/9781845690151.256>
- [25] ASTM D5587-15, *Standard Test Method for Tearing Strength of Fabrics by Trapezoid Procedure*. West Conshohocken, PA, USA: ASTM International, 2019.
- [26] M. Martínez-Estrada, I. Gil, and R. Fernández-García, "An alternative method to develop embroidery textile strain sensors," *Textiles*, vol. 1, no. 3, pp. 504-512, 2021.  
<https://doi.org/10.3390/textiles1030026>
- [27] Y. Zheng, Y. Li, Y. Zhou, K. Dai, G. Zheng, B. Zhang, ... and C. Shen, "High-performance wearable strain sensor based on graphene/cotton fabric with high durability and low detection limit," *ACS Appl. Mater. Interfaces*, vol. 12, no. 1, pp. 1474-1485, 2019.  
<https://doi.org/10.1021/acsami.9b17173>
- [28] Z. A. Abro, Z. Yi-Fan, C. Nan-Liang, H. Cheng-Yu, R. A. Lakho, and H. A. Halepoto, "A novel flex sensor-based flexible smart garment for monitoring body postures," *J. Ind. Text.*, vol. 49, no. 2, pp. 262-274, 2019.  
<https://doi.org/10.1177/1528083719832854>
- [29] B. A. Kuzubasoglu, E. Sayar, C. Cochrane, V. Koncar, and S. K. Bahadir, "Wearable temperature sensor for human body temperature detection," *J. Mater. Sci.: Mater. Electron.*, vol. 32, no. 4, pp. 4784-4797, 2021.  
<https://doi.org/10.1007/s10854-020-05217-2>
- [30] A. Al Dahoud and M. Fezari, *NodeMCU V3 for Fast IoT Application Development*, Notes, vol. 5, 2018.